Mol Breeding (2019) 39: 106
https://doi.org/10.1007/s11032-019-1000-9

Construction of the first high-density genetic map and QTL mapping for photosynthetic traits in *Lycium barbarum* L.

Haiguang Gong · Fazal Rehman · Tianshun Yang · Zhong Li · Shaohua Zeng · Lizhu Pan · Yongqing Li · Ying Wang

Received: 13 February 2019 / Accepted: 29 May 2019 / Published online: 6 July 2019

Abstract Photosynthesis is essential for plant development as well as crop yield. QTL mapping was conducted for photosynthetic traits such as net photosynthetic rate (P_N), stomatal conductance (Cond), inner-cellular carbon dioxide (Ci), transpiration rate (Trmmol), limiting value of the stoma (Ls), and water use efficiency (WUE). A high-density genetic map covering 964.03 cM was developed based on a hybrid population of the Goji (*Lycium barbarum* L.). The genetic map consisted of 23,967 markers with an average distance of 0.040 cM between two adjacent markers. Twenty-nine and three quantitative trait loci (QTLs) for photosynthetic traits and trunk diameter (TD), respectively, were detected, of which 8 QTLs, including 3 for P_N, 2 for Cond, 1 for Trmmol, 1 for Ci, and 1 for Ls, can be detected in at least 2-year measurements (from 2017 and 2018, as well as the averaged data from 2017 and 2018, which was regarded as a 3rd year, named 1718). Among these measurements, qP_N1 was detected in all 3 years and considered a stable QTL whereas qLs1 and qLs2 with the highest phenotypic variance explained (PVE%) 32.012 and 17.965 were detected as major QTLs. P_N, Cond, Ci, Trmmol, Ls, and WUE showed significant correlations with each other except for Cond and WUE whereas P_N and Cond were significantly correlated with TD ($P < 0.05$). These findings indicate that P_N and Cond are critical factors for the growth of plants and QTLs contribute to P_N, Cond, and TD, which could provide an improved way to enhance the breeding of the Goji in relation to its growth rate.

Keywords Genetic map · ddRAD-seq · QTL mapping · Goji berry · Photosynthesis

Haiguang Gong and Fazal Rehman contributed equally to this work.

Electronic supplementary material The online version of this article (https://doi.org/10.1007/s11032-019-1000-9) contains supplementary material, which is available to authorized users.

H. Gong · F. Rehman · T. Yang · S. Zeng · L. Pan · Y. Li · Y. Wang (✉)
Key Laboratory of South China Agricultural Plant Molecular Analysis and Genetic Improvement, Guangdong Provincial Key Laboratory of Applied Botany, South China Botanical Garden, Chinese Academy of Sciences, Guangzhou 510650, People's Republic of China
e-mail: yingwang@scib.ac.cn

H. Gong · F. Rehman · Y. Li · Y. Wang
University of Chinese Academy of Sciences, Beijing 100049, People's Republic of China

Z. Li
Bairuiyuan Company, Yinchuan, Ningxia 750000, People's Republic of China

S. Zeng
GNNU-SCBG Joint Laboratory of Modern Agricultural Technology, Gannan Normal University, Ganzhou, Jiangxi 341000, People's Republic of China

Introduction

Goji (*Lycium barbarum* L.) is one of the most important medicinal plants in China, Europe, and the Mediterranean region (Amagase and Farnsworth 2011; Li et al. 2012; Zhao et al. 2015). Goji has red fleshy fruits that

have affinal drug and diet functions and contain trace minerals including zinc, iron, calcium, and phosphorus and abundant amino acids as well as metabolic compounds such as flavonoids, carotenoids, and polysaccharides (Qiu et al. 2014; Wang et al. 2010a, 2010b; Yin and Dang 2008). Studies have revealed that antioxidative compounds, polysaccharides (Dahech et al. 2013), and hydroxycinnamic acid amides (HCCA) have potential anti-inflammation effects (Wang et al. 2017). Goji berry also has a great effect on reversing neurodegeneration in Alzheimer's patients and relieving symptoms (Chang et al. 2015). Due to its suitable semi-arid climate and particular geographic position, Ningxia province in China should be considered as a "daodi" area of the goji: a zone that can cultivate goji with stable growth, premium quality, and efficient production. In fact, China is the primary producer and exporter in the world. The recent production estimates of goji in China is 88,000 ha covering entire Ningxia region including Xinjiang, Gansu, Inner Mongolia, Hubei, Shanxi, and northwest to central China (Chen et al. 2018). By 2017, the yield of dry goji berries in China accounted for 410,608 t while in Ningxia Region, which is considered the biggest planting area of goji, the yield is estimated to be about 108,473 t of goji (SFAC 2018). Goji is a privileged tree; its fruit has many advantages: provides cures to the number of health-related issues such as neurological, cardiovascular, gastrointestinal regularity, and anti-aging (Chen et al. 2018). As the domestic and international market demand rises, the production in Ningxia Province cannot meet the consumer demand (Yao et al. 2018). Thus, it is necessary to enhance the production of the goji berry in more suitable cultivation regions.

Photosynthetic pigments such as chlorophyll affect photosynthetic efficiency. Net photosynthesis (P_N) plays a positive role in plant growth, biomass accumulation, and crop yield, and shows genetic inheritance differences in different environments (Qu et al. 2017; Zelitch 1982). In modern agriculture, photosynthesis is not utilized efficiently and is far from its biological limit, but it can serve as a key player to improve the genetic production potential of crops (Long et al. 2015).

Cultivating a high or sustained stomatal conductance (Cond) is an indirect way to improve crop yields (Richards 2000). A high stomatal conductance is critical for crop growth and yield, particularly during the period of seed formation and filling (Roche 2015). Stomata are the main gateway for leaves to absorb CO_2 and water for photosynthesis. The photosynthesis process takes place during the daytime with the stomata opening, and the stomatal conductance is a critical limitation to the photosynthetic rate (Roche 2015).

Cellular CO_2 concentration (Ci) is another factor that affects photosynthetic traits. However, the stomatal limitation is revealed by the difference between the external carbon dioxide and cellular carbon dioxide, which is closely associated with the exchange capability of the stoma. Under a mild water deficit, stoma closure causes the stomatal limitation of photosynthesis, which leads to a decline in photosynthesis (Mullet and Whitsitt 1996; Pinheiro et al. 2004). The water use efficiency (WUE) is closely related to drought tolerance with the combined effect of a deep root system. In fact, more WUE contributes to high drought tolerance (Hund et al. 2009). The trunk diameter (TD) is closely correlated with the weight of different internal organs of shrubs, which collectively represent the biomass of plants (Harrington 1979).

To develop a cultivar with an efficient photosynthetic system, marker-assisted selection (MAS) provides an innovative and efficient way for species selection and variety development (Singh and Singh 2015). The recent sequencing techniques such as next-generation sequencing (NGS) and the use of restriction enzymes called reduced representation genome sequencing (RRGS) provide an efficient way to discover the SNP locus and enable high-density genetic map construction for QTL mapping (Baxter et al. 2011; Davey et al. 2011; Wang et al. 2012; Migicovsky and Myles 2017). Under NGS, there are several RRGS-based sequencing techniques that have been developed for genetic map construction, including SLAF-seq (Sun et al. 2013), double-digest restriction site-associated DNA sequencing (ddRAD-seq) (DaCosta and Sorenson 2016), restriction site-associated DNA sequencing (RAD-seq) (Zhu et al. 2018), and genome-wide association studies (GWAS) (Han et al. 2018). ddRAD-seq is a type of genotyping-by-sequencing (GBS) method using double-enzyme digestion, yielding a large scale of SNP markers and InDel polymorphisms (DaCosta and Sorenson 2016). ddRAD-seq has been applied in different flora and fauna species to construct genetic map such as the Japanese eel, bighead carp, peanut, *Brassica napus*, Chinese cabbage, and Coho salmon (Barria et al. 2018; Fu et al. 2016; Kai et al. 2014; Laila et al. 2019; Zhou et al. 2014).

The primary goals of this research were to construct the genetic map based on genotyping of goji F1

population, then to investigate the relationship between 6 photosynthetic traits and trunk diameter (TD) by QTL mapping analysis and to provide a direction for the future breeding of goji. With these aims, an intraspecific hybridized F1 population has been established based on "Ningqi5" and "Zhongkeluchuan1" (two cultivars of *Lycium barbarum* L.). ddRAD-seq was exploited to identify SNP markers and constructed a high-density genetic map of *L. barbarum* and QTL mapping was performed based on the photosynthetic data collected during 2017 and 2018.

Materials and methods

Plant materials

Two cultivars of *L. barbarum* "Ningqi-5" as the female parent (N5) and "Zhongkelüchuan-1" (ZKLC1) as the male parent were cross-fertilized in August 2016 (the parents N5 and ZKLC1 images have been added in Supplementary File 1, Fig. S4). The seeds were sown in the greenhouse during the spring of 2017, and then in May transplanted to a field at the Northwest China Bio-agricultural Center, Yinchuan City, Ningxia Province, China. In September of 2017, a total of 305 randomly chosen offspring were defined as the F_1 population for this study.

DNA extraction and library construction and sequencing

The young leaves from the parents as well as progeny were collected and dried with desiccant (silica gel) prior to DNA extraction. All the leaves were extracted with the cetyl-trimethyl-ammonium bromide standard method (CTAB method) with minor modifications (Murray and Thompson 1980). ddRAD-seq was used to genotype the F_1 population and their parents according to (Wu et al. 2016) with minor modifications. The procedure framework adopted was as follows: (1) 500-ng high-quality genomic DNA was digested into fragments with two restriction enzymes "SacI and MseI"; (2) the adaptors "SacAD and MseAD" with unique barcodes were ligated with the DNA fragments; (3) the DNA fragments were separated on 2% agarose gel and the length range from 320 to 420 bp was chosen for amplification before sequencing on an Illumina Hi-seq platform. The original paired-end sequence length was 150 bp (Wu et al. 2016).

SNP marker development and genetic map construction

All the raw sequences were screened by Cutadapt (v1.13) (Chen et al. 2017a) and Trimmomatic (v 0.36) (Brauer et al. 2017) software to obtain clean reads. All clean reads were used to developed polymorphic markers with Stacks (v1.48) (Rochette and Catchen 2017). The polymorphic markers were filtered with MAF ≥ 0.1 and missing rate of ≤ 0.25 values (Catchen et al. 2011). Only the ddRAD markers were screened and identified in more than 75% of the progenies with $\leq$ 25% missing values, while a minor allele frequency (MAF) greater than 0.1 was used as a standard for the genetic map construction with Lep-MAP (v.3.0) (LOD > 47) (Rastas 2017).

Phenotypic trait measurement

In September of 2017 and 2018, the phenotypic traits related to photosynthesis were measured daily from 9:00 a.m. to 12:00 a.m. The net photosynthetic rate (P_N, μmol CO_2 s^{-1} m^{-2}), transpiration rate (Trmmol, mmol H_2O m^{-2} s^{-1}), intercellular CO_2 concentration (Ci, μmol CO_2 mol^{-1}), stomatal conductance (Cond, mmol H_2O s^{-1} m^{-2}), and ambient CO_2 concentration (Ca, μmol CO_2 mol^{-1}) were measured using a Li-6400 (LI-COR, Lincoln, NE USA) with a photosynthetic active radiation of 1000 μmol m^{-2} s^{-1} and an air flow rate of 500 μmol/s. The data were collected with three replicates from each plant, and the average values were used. The limiting value of the stomata (Ls) and water use efficiency (WUE) were calculated using the formulas Ls = 1-Ci/Ca and WUE = P_N/Trmmol (Chen et al. 2006). Due to variation in the weather conditions, all the data were collected within 10 days. The trunk diameter (the stem diameter 10 cm above the ground) of the F_1 individuals was also measured with a vernier caliper in August of 2018 (Niklas 1995). After deleting the missing data, the 6 photosynthetic traits were analyzed using a Pearson correlation between 2 years with SPSS v21.0 (Sanchez-Perez et al. 2012). The correlation of 7 traits (averaged data between 2017 and 2018 of P_N, Cond, Ci, Trmmol, Ls, WUE, and the TD of 2018) was also analyzed using Past software (v.3.0, University of Oslo, Norway).

QTL mapping

The QTL mapping for the average of the 7 phenotypic traits (P_N, Trmmol, Ci, Cond, Ls, WUE, and TD) was performed using the software GACD (v.1.0, Chinese Academy of Agricultural Sciences, CAAS, Beijing, China) (Zhang et al. 2015). All the missing phenotypic data were deleted while performing inclusive composite interval mapping (ICIM) and a logarithm of odds (LOD) of 2.5 was selected as a threshold to determine the QTL. A QTL with explained phenotypic variation (EVP%) > 10 observed as a major QTL whereas detection in all 3 years defined as a stable QTL (Che et al. 2018). The genetic map and QTLs were graphed out by Mapchart (v. 2.2) (Akond et al. 2013).

Results

Analysis of ddRAD-seq data and genetic map construction

A total of 615.83 Gb raw data were obtained after the ddRAD library construction and next-generation sequencing with high base quality standard Q20 (98.54%) and Q30 (95.53%). The average GC contents were 41.47% with the corresponding sequencing depths 16.30 and 17.52, and the read numbers 4,138,487 and 5,737,731 for the parents N5 and ZKLC1, respectively. These paired-end reads produced 249,284 and 283,424 tags of 150 bp in length. F_1 individual's average read numbers were 7,484,038 with a tag production rate of 4.64% (Fig. S1, Supplementary File 5). As the F1 intraspecific population based on N5 as female and ZKLC1 as male was highly heterozygous, both parents exhibited a wide range of variations in genomic contents as well as agronomic traits. Thus, during the distribution of markers into population segregation pattern, only heterozygous groups were considered and homozygous group abandoned. A total of 26,860 markers were confined into seven segregation patterns by using Stacks software, which further split as 11,639, 8145, 3940, 1706, 767, 555, and 108 markers into lmxll, nnxnp, hkxhk, efxeg, abxcc, ccxab, and abxcd segregation groups, respectively, with 7.74% marker producing rate (Table S1, Supplementary File 5).

A total of 26,860 markers were used by the software Lep-MAP (v.3) (LOD > 47), and a consensus map of 23,967 markers was constructed with a total length of 964.03 cM and 2740 bins were obtained (Fig. 1; Table 1; Supplementary File 6). The mapping ratio of the markers was 89.23%, of which the N5 (female parent) and ZKLC1 (male parent) maps had lengths of 886.75 cM and 1042.38 cM, respectively. The average marker interval for N5 was 0.038 cM with a maximum interval of 4.610 cM (Supplementary Fig. S2 and Files 1 and 7). In the male map (ZKLC1), the mean markers and the maximum distance were 0.042 cM and 6.60 cM, respectively (Supplementary Fig. S3 and Files 1 and 7). Both the N5 and ZKLC1 maps consisted of 13 linkage groups. However, the markers in LG12 had no exchange in the N5 map, while those in LG13 had also no exchange in the ZKLC1 map as well. The mean and maximum marker interval was 0.040 cM and 3.61 cM for the consensus map with an average of 1844 markers, respectively (Table 1). The densest one was the LG1 with total 3219 markers, 0.023 cM mean interval distance, and the maximum interval distance of 0.331 cM. The less dense was LG11 with 1327 markers, 0.081 cM mean interval distance, and the maximum interval distance of 2.46 cM.

Genetic map evaluation

The quality of the consensus genetic map was evaluated with a haplotype map as well as a heat map (Xu et al. 2015; Zhu et al. 2015). Eleven linkage groups of the genetic map with exchangeable markers were evaluated by the recombination rate between the markers under each linkage group in the heat map (Supplementary File 2). The integrated map quality was evaluated by pairwise recombination rate of markers, which were used to construct the heat maps. The rate of recombination and the genetic distance between two markers were evaluated to define the accuracy of the mapping. The vertical and horizontal coordinates represented the corresponding markers in the linkage groups. Blue square revealed low recombination rate, while red one indicated a high rate of recombination. A heat map can be applied to examine the possibility of order error by the test of markers recombination rate if the exchange rate is not gradual between the markers and the corresponding linkage group. The population genotyping error and the double exchange were revealed by haplotype mapping (Zhu et al. 2015). The haplotype map was constructed for 305 F1 individuals and their parents as a control using 23,967 markers. Each individual recombination event was represented in the haplotype map clearly (Supplementary File 4) and showed no missing or

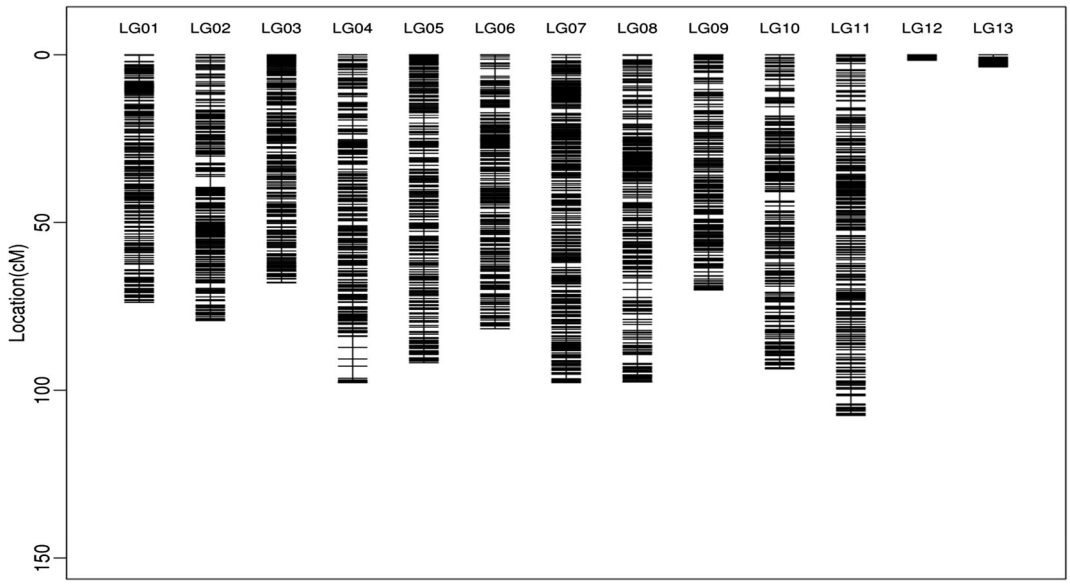

Fig. 1 Marker distributions of a consensus map of *L. barbarum*

crossover in the 11 linkage groups. According to two kinds of maps, all the linkage groups distributed evenly, which further confirm the suitability of the F1 population for genetic mapping analysis.

Phenotypic trait evaluation

The six phenotypic traits related to photosynthesis (P_N, Cond, Ci, Trmmol, Ls, and WUE) of two parents were measured in 2 years and analyzed by one-way ANOVA using the statistical software SPSS (v21.0). The results indicated that five traits of the two parents were highly significantly different ($P < 0.01$) for the 2017–2018 data (Table 2), while WUE was significantly different ($P < 0.05$) in 2017 and highly significantly different ($P < 0.01$) in 2018. ZKLC1 was extremely significantly higher ($P < 0.01$) than N5 in P_N, Cond, Ci, and Trmmol and highly significantly lower ($P < 0.01$) in Ls during

Table 1 Basic characteristics of consensus map of *L. barbarum*

Linkage group ID	Length (cM)	No. markers	No. bins	Marker interval (cM)	Bin interval (cM)	Max interval (cM)
LG01	73.77	3,219	224	0.023	0.331	1.81
LG02	79.19	2,827	230	0.028	0.346	3.29
LG03	68.04	2,580	233	0.026	0.293	1.15
LG04	97.73	2,395	238	0.041	0.412	3.61
LG05	91.81	2,129	259	0.043	0.356	1.64
LG06	81.64	1,928	233	0.042	0.352	2.3
LG07	97.71	1,898	317	0.052	0.309	1.48
LG08	97.55	2,309	252	0.042	0.389	2.63
LG09	70.17	1,486	199	0.047	0.354	1.8
LG10	93.62	1,290	251	0.073	0.374	2.79
LG11	107.55	1,327	274	0.081	0.394	2.46
LG12	1.64	353	11	0.005	0.164	0.17
LG13	3.61	226	19	0.016	0.19	0.66
Average	74.16	1,844	211	0.040	0.328	1.98
Total	964.03	23,967	2,740	–	–	–

Table 2 Analysis of variance (ANOVA) of six traits between N5 and ZKLC1

Traits	2017		2018	
	N5	ZKLC1	N5	ZKLC1
P_N	9.20 ± 1.47**	18.19 ± 2.13**	10.35 ± 1.15**	16.45 ± 1.76**
Cond	0.12 ± 0.05**	0.48 ± 0.08**	0.12 ± 0.03**	0.36 ± 0.08**
Ci	245.19 ± 35.75**	312.26 ± 5.65**	229.93 ± 16.12 **	287.03 ± 21.88**
Trmmol	3.03 ± 1.17**	8.45 ± 0.84**	5.07 ± 1.19 **	11.88 ± 0.97**
Ls	0.39 ± 0.09**	0.21 ± 0.01**	0.41 ± 0.04 **	0.25 ± 0.06**
WUE	3.29 ± 0.87*	2.16 ± 0.21*	2.09 ± 0.23 **	1.38 ± 0.09**

**N5 and ZKCL1 have extremely significant differences in this trait of the same year ($P < 0.01$)

*N5 and ZKLC1 have significant differences in this trait of the same year ($P < 0.05$)

2017–2018. For the trait of WUE, N5 was significantly higher than ZKLC1 ($P < 0.05$) in 2017 and extremely significantly higher in 2018 ($P < 0.01$). The frequency histogram of the six photosynthetic traits showed a pyramid distribution with regularity in the values of the parents (Fig. 2). By the Pearson correlation of all individuals analyzed between 2017 and 2018 of the six traits, P_N, Cond, and Trmmol showed extremely significant correlations ($P < 0.001$), while Ci, Ls, and WUE non-significant (Table 3). The six photosynthetic traits exhibited significant correlations with each other ($P < 0.05$), except for Cond with WUE ($P > 0.05$). Among these photosynthetic traits, P_N and Cond had significant correlations with TD (Fig. 3).

QTL mapping

The photosynthetic trait data were collected from 2017 to 2018, and the averaged of the 2 years was treated like the third-year 1718 data. The genetic map and data of the 6 photosynthetic traits were used for the analysis by using GACD (v.10), and 1000 permutation tests and a LOD score of 2.5 were selected as the thresholds for the QTL analysis. A total of 32 QTLs with six photosynthetic traits and TD were identified. Among them, 8 QTLs were identified based on 2 years of data (out of 2017, 2018, & the averaged data of the 2 years). For the net photosynthetic rate, the QTLs were mapped on chromosomes 3 and 5, with LOD scores ranging from 3.22 to 5.28 among which the QTL "qP_N1" had the highest LOD score of 5.28 and detected in 3 years of data (Table 4). Thus, qP_N1 was regarded as a stable QTL. The phenotypic variance explained by the individual QTLs of the photosynthetic rate was within 5.16 and 7.03, and QTL qP_N1 was mapped to chromosome 3. In total, the LOD scores were found to be in the range between 2.50 and 20.21. The phenotypic variance explained by the individual QTLs for the photosynthesis-related traits was between 3.17 and 32.01, whereas for the other traits such as Cond, Ci, Trmmol, and Ls, only five QTLs were detected based on 2 years of data (2017, 2018, & the averaged of the 2 years 1718). qLs1 and qLs2 with the highest EVP% 32.012 and 17.965, respectively, can be identified as major QTLs. Fourteen QTLs of different traits were found to overlap at five different locations on the linkage group. The four QTLs of $_qP_N1$, Cond2, qTrmmol2, and qLs1 were located at the same position 26.39–27.38 cM on LG3. The 6 QTLs of qCi, qLs4, qWUE2, qP_N2, qCond3, and qLs5 were also found at the same positions of 1.64–2.13 cM on LG2 and 30.98–31.64 cM on LG3, respectively. The other two overlapping QTLs comprised of P_N and Cond. All four QTLs of P_N overlapped with Cond (Table S2). The additive effect of the female (N5) contributing to the 29 QTLs ranged from − 0.493 to 5.323, while that of the male parent (ZKLC1) was from − 5.450 to 0.662. The dominant effect of both parents ranged from − 0.197 to 3.717. The additive effect of most of the QTLs was found low.

Discussion

Construction of the genetic map

Genetic map construction and QTL mapping is a highly efficient way to analyze traits in plants (Li et al. 2014). So far, to our knowledge, there has been no report on the

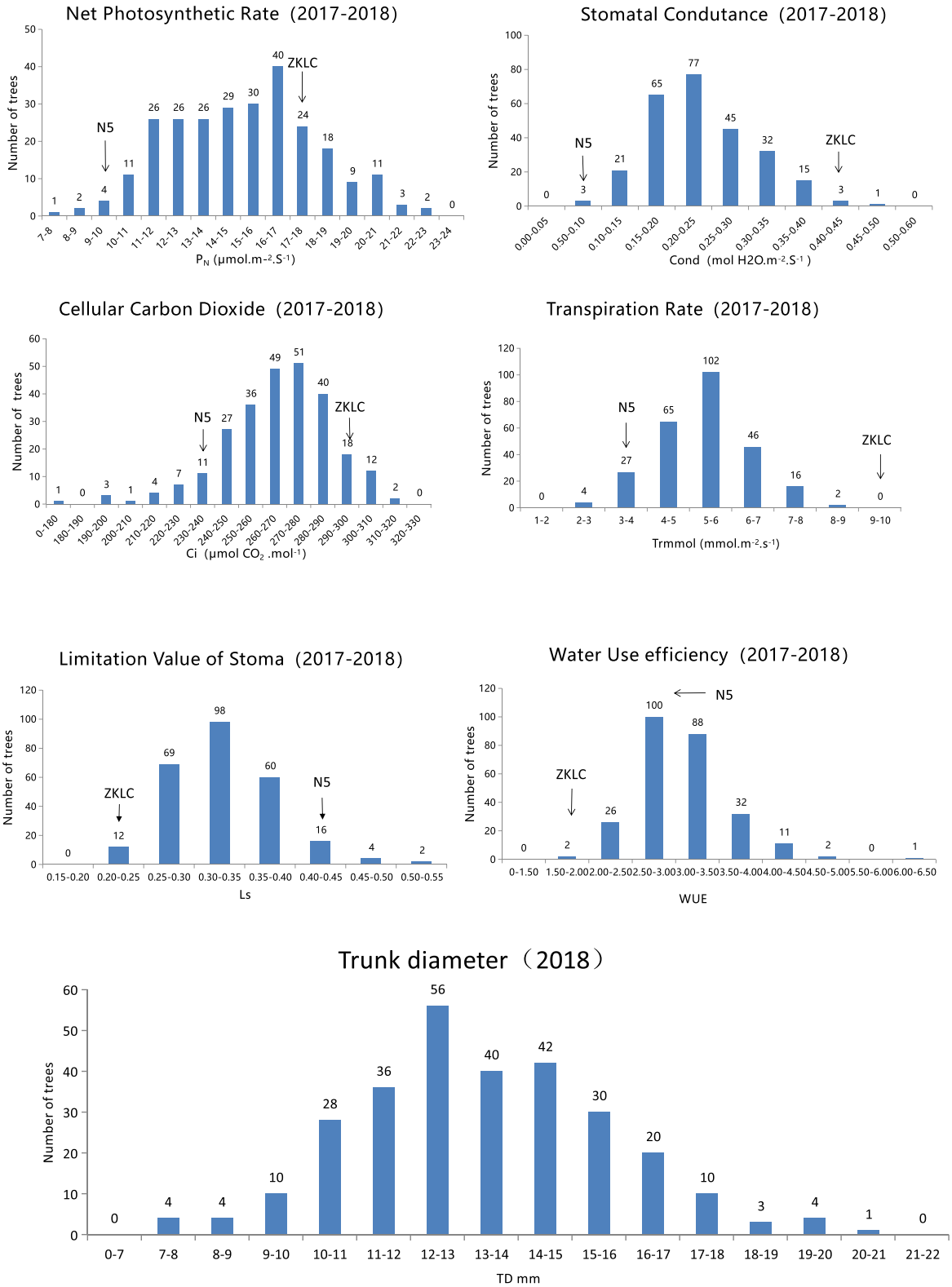

Fig. 2 Frequency distribution of 6 photosynthetic traits and trunk diameter for F1 population. Each *x*-axis represents the value of one of the 7 traits, and the *y*-axes indicate the number of trees with the corresponding value on the *x*-axis. Arrows show the values of the female parent (N5) and the male parent (ZKLC1)

Table 3 Correlation between each of the six traits in 2017 and 2018 among all individuals

Trait	2017			2018			Correlation between 2 years
	Mean	Maximum	Minimum	Mean	Maximum	Minimum	*P* value
P_N	15.04 ± 3.09	22.74	6.34	15.18 ± 2.94	23.19	8.09	*P* < 0.001
Cond	0.24 ± 0.08	0.59	0.05	0.23 ± 0.08	0.54	0.05	*P* < 0.001
Ci	254.25 ± 22.39	304.10	190.61	277.25 ± 38.25	347.64	90.71	*P* > 0.05
Trmmol	6.25 ± 1.48	10.17	2.15	4.39 ± 1.20	8.53	1.41	*P* < 0.001
Ls	0.34 ± 0.06	0.53	0.21	0.32 ± 0.09	0.78	0.14	*P* > 0.05
WUE	2.48 ± 0.49	4.11	1.36	3.66 ± 0.88	7.33	1.56	*P* > 0.05

genetic map of *Lycium barbarum* L. published yet, although EST-SSR markers have been developed for the construction of the genetic map of *Lycium barbarum* L. (Chen et al. 2017b). The genetic map in the current study is regarded as the first genetic map of *Lycium barbarum* L.. Compared to RAD-seq, ddRAD-seq has numerous advantages over previous sequencing techniques, as it is a cost-effective, efficient, and rapid method to obtain a greater number of reads with robustness and unique barcode system (Peterson et al. 2012; Kai et al. 2014). It is applicable to those species without reference sequence genome and use of double restriction enzyme digestion concurrently results in reduced library construction (Peterson et al. 2012). And a greater number of SNPs are generated than using RAD-seq (Kakioka et al. 2013). Thereby, ddRAD-seq has been employed to construct the genetic map of many species including the Japanese eel (Kai et al. 2014), strawberry (Davik et al. 2015), lotus (Liu et al. 2016), tomato (Liu et al. 2016), linseed flax (Zhang et al. 2018), and peanut (Wang et al. 2018). Hence, the ddRAD library is a reliable method for high-density genetic map construction. A total of 26,860 markers from 347,070 tags were obtained with a 7.74% marker producing rate. The seven segregation patterns and 23,967 markers obtained after filtering out the repetitive or distorted markers were distributed as 11,639 (lmxll), 8145 (nnxnp), 3945 (hkxhk), 1706 (efxeg), 767 (abxcc), 555 (ccxab), and 108 (abxcd). The results demonstrated that goji is a highly heterozygous tree plant with a high level of

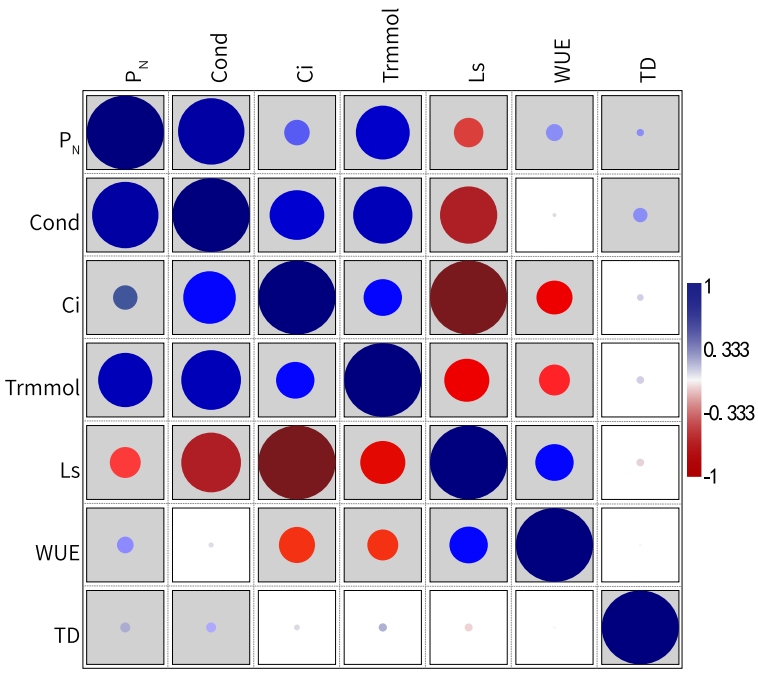

Fig. 3 Correlation test among six photosynthetic traits and trunk diameter (TD). *Red circles indicate that the two traits have a negative correlation, and blue means a positive correlation. Square boxes indicate that the correlation of the traits is significant ($P < 0.05$)

Table 4 Summary of QTLs for photosynthetic trait and TD in F1 population of *L. barbarum*

Trait	QTL	Year	LG ID	Position	IC (cM)	LOD	PVE (%)	Parental effect		
								M	F	FM
P_N	qP_N1	2017	3	27	26.39–27.38	5.28	7.028	− 0.833	− 0.041	0.022
		2018	3	27	26.39–27.38	3.22	4.780	− 0.638	0.141	− 0.011
		1718	3	27	26.39–27.38	4.23	6.324	− 0.711	0.207	0.024
	qP_N2	2017	3	31	30.98–31.64	5.00	6.615	0.115	0.809	− 0.094
	qP_N3	2018	3	51	50.33–51.31	3.47	5.174	− 0.210	0.622	− 0.157
		1718	3	51	50.33–51.31	4.04	6.099	− 0.078	0.708	− 0.197
	qP_N4	2018	5	85	84.6–85.09	3.82	5.688	0.662	− 0.228	0.065
		1718	5	85	84.6–85.09	3.45	5.159	0.647	− 0.081	0.142
Cond	qCond1	2017	2	21	20.66–21.15	2.59	3.378	0.007	0.008	0.012
	qCond2	2017	3	27	26.39–27.38	4.60	6.298	− 0.021	− 0.001	− 0.003
	qCond3	2017	3	31	30.98–31.64	3.65	4.935	0.005	0.019	− 0.004
	qCond4	2017	5	85	84.6–85.09	3.54	4.819	0.018	0.001	0.006
	qCond5	2018	3	51	50.33–51.31	2.86	4.771	− 0.008	0.016	− 0.001
		1718	3	51	50.33–51.31	3.89	6.444	− 0.004	0.017	− 0.003
	qCond6	2018	5	63	62.79–63.28	2.68	4.324	0.010	0.001	0.015
		1718	5	63	62.79–63.28	2.79	4.500	0.014	0.000	0.005
Trmmol	qTrmmol1	2017	3	11	10.33–11.15	2.72	3.60	0.042	0.272	0.004
	qTrmmol2	2017	3	27	26.39–27.38	7.10	9.663	− 0.444	0.049	− 0.076
		1718	3	27	26.39–27.38	4.66	7.519	− 0.245	0.156	0.000
	qTrmmol3	2017	7	4	3.93–4.1	2.50	3.166	− 0.053	0.251	0.015
	qTrmmol4	2018	3	50	49.84–50.17	2.93	4.840	− 0.185	0.182	0.038
	qTrmmol5	2018	6	23	22.95–23.28	2.88	4.766	0.245	0.077	0.094
	qTrmmol6	1718	2	51	50.99–51.16	2.66	4.108	0.015	0.157	− 0.127
	qTrmmol7	1718	3	15	14.92–16.07	2.51	3.903	0.058	0.209	− 0.039
	qTrmmol8	1718	5	86	85.74–86.07	3.06	4.710	0.179	− 0.030	0.140
	qTrmmol9	1718	10	10	10.00–10.17	3.03	4.896	0.021	0.227	0.076
Ci	qCi	2018	10	2	1.64–2.13	2.72	4.530	− 5.450	5.323	3.717
		1718	10	2	1.64–2.13	4.39	7.438	− 3.949	4.229	3.274
Ls	qLs1	2017	3	27	26.39–27.38	20.21	32.012	0.032	− 0.009	0.000
	qLs2	2017	3	33	32.62–33.12	11.93	17.965	− 0.024	− 0.010	0.002
	qLs3	2017	7	48	47.21–48.03	2.71	3.825	− 0.012	0.000	0.001
	qLs4	2018	10	2	1.64–2.13	3.07	5.099	0.014	− 0.014	− 0.008
		1718	10	2	1.64–2.13	4.46	7.555	0.010	− 0.011	− 0.007
	qLs5	1718	3	31	30.98–31.64	2.77	4.738	0.002	− 0.009	− 0.007
WUE	qWUE1	2017	7	65	64.92–65.08	2.89	4.401	− 0.091	− 0.005	− 0.034
	qWUE2	2018	10	2	1.64–2.13	2.61	4.317	0.104	− 0.162	− 0.016
	qWUE3	1718	4	34	32.63–34.1	3.48	5.949	− 0.028	0.054	− 0.111
	qWUE4	1718	6	0	0.00–0.16	2.50	4.089	0.006	− 0.078	− 0.070
TD	qTD1	2018	3	67	66.89–67.87	4.20	5.928	− 0.543	0.147	0.062
	qTD2	2018	5	88	87.55–88.2	3.25	4.550	0.453	0.244	0.044
	qTD3	2018	6	38	37.38–38.2	3.65	5.093	0.225	− 0.493	0.043

**LG ID*, linkage group ID; *PVE%*, phenotypic variation explained; parental effects F and M are the additive effects of the female (N5) and male parents (ZKLC1), respectively. FM indicates the dominant effect of both parents

DNA polymorphism, heterozygosity value for goji ranged from 0.00 to 1.00 with 0.439 as average (Zhao et al. 2010). Thus, it was feasible to construct a genetic map of *Lycium barbarum* L. based on the F_1 population.

A high-density genetic map connects the traits and genome, thereby providing a scaffold for the genome to anchor a sequence into the chromosomes (Gong et al. 2016). For SNP markers, if the accuracy of the selection reaches 0.86, the average interval between two adjacent markers needs to be 0.125 cM (Solberg et al. 2008). A low-density genetic map has low efficiency and accuracy in detecting QTLs (Li et al. 2014). The integrated genetic map in the current study consisted of 23,967 markers, covering 964.03 cM with an average marker interval distance of 0.04 cM. Comparatively, this density is much higher than 0.16 cM, the average distance between adjacent markers in pepper genetic map (Li et al. 2018). The DNA contents of *L. barbarum* is 4.35 Pg/2C (Chen et al. 2013), and the average physical to genetic distance ratio in goji was 2256 kb/cM. The average amount of DNA between two adjacent markers was 90,750 bp, quite lower than 200,000 bp, the hot spot DNA contents described by Yunbi Xu (Xu 2010) likewise in other species such as the 676,000 bp and 606,000 bp in two parent map of the grape (Chen et al. 2015) and 130,000 bp in maize (Chen et al. 2014). QTL mapping and genetic mapping analysis in grapes and other crop species (Chen et al. 2015) provide evidence that the current genetic map can be used for QTL mapping of agriculturally important traits.

Photosynthetic traits and biomass-related traits

The photosynthetic traits and water use efficiency are the basic factors for plants to guarantee its yield and production, especially during dry conditions. P_N, Ci, and WUE can be co-located on the same QTL as the grain yield and yield components in wheat (Xu et al. 2017). The maximum photosynthetic rate and stomatal conductance affect the ultimate yield (Richards 2000). The transpiration rate has a direct link with the water-conservation trait. Drought is a critical factor of crop yield losses in dry areas, and there has been no report of improving the water-conservation traits of crops to lower the consequences of drought on crop yield (Sinclair 2017). For the sunflower, 19 photosynthesis-related QTLs were detected, including three P_N, four Cond, three Trmmol, and one Ci-related QTL (Herve et al. 2001). Fourteen photosynthetic traits were found in rice including five P_N, two Cond, three Trmmol, and four Ci-related QTLs (Zhao et al. 2008). Wheat crops are grown under water sufficient and drought environmental conditions for 2 years showed that 12, 9, 14, 8, and 14 QTLs contributed to the photosynthetic traits of P_N, Cond, Ci, Trmmol, and WUE, respectively (Xu et al. 2017). The QTLs were categorized into five different types, including non-specific QTLs, trait-specific QTLs, stage-specific QTLs, genotype-specific QTLs, and environment-specific QTLs. Among these four types of QTLs, only the non-specific has robustness in different development stages and different environments (Liu et al. 2008). In the current research work, a total of 32 QTLs contributed six photosynthetic traits and trunk diameter (TD). Among these QTLs, qP_N1 was detected in three datasets, while qP_N3, qP_N4, qCond5, qCond6, qTrmmol2, and qLs4 overlapped in two datasets of detection. Thus, qP_N1 can be regarded as a non-specific QTL, while the other 17 QTLs were environment-specific QTLs. Due to the complex effects, the trait-specific, stage-specific, genotype-specific, and environment-specific QTLs are changeable and can only be detected in specific environments (Liu et al. 2008). The six photosynthetic traits and TD showed a pyramid frequency distribution, and the parents were distributed regularly. The result was in agreement with that found in rice (Liu et al. 2008) and grapes (Chen et al. 2015). Based on the correlation analysis, P_N and Cond have significant positive correlations with TD. Our results corresponding to those from a photosynthetic study on rice (Qu et al. 2017). It is reported that photosynthetic traits can be mapped in the same QTLs (Xu et al. 2017), and P_N, Cond, and Trmmol can have overlapping QTLs in rice (Zhao et al. 2008). These statements are in agreement with our results that P_N, Cond, Trmmol, and Ls were co-located in the same QTL. The other four QTLs contributed at least two photosynthetic traits.

Two extreme short linkage groups detected in the consensus map

A genetic map is constructed according to the recombination frequency between markers, and recombination occurs in synapsis during the tetrad period (Xu 2010). Thus, the synapsis of homologous chromosomes is an important factor to construct linkage groups in the genetic map. There are 12 pairs of chromosomes in *L. barbarum* (2n = 24) (Chen et al. 2013). However, according to our results, the genetic map was

constructed with 13 linkage groups, among which the 12th one has no marker exchange for the N5 map, while the 13th one has also no marker exchange for the ZKLC1 map as well. In the same context, the linkage group size was quite short for the 12th and 13th LG with 353 and 226 number of markers, respectively. Therefore, the undetected recombination was the primary reason for the extreme short genetic distances of these two linkage groups.

The possible reasons for this result, based on the previous reports, might be that Ningqi-5 is a male sterile line, and the pollen development is blocked in the tetrad period during meiosis (Li et al. 2013). In *Drosophila*, a single gene is responsible for male sterility and causes segregation distortion (Phadnis and Orr 2009). The sterile mutation can also block the oogenesis or alter its morphology (Schupbach and Wieschaus 1991). Chromosome irregularity may also cause induced germinal changes (Stadler 1931). Therefore, the segregation distortion of markers happened in one chromosome of each parent.

Conclusion

In this study, we constructed the first high-density genetic map of *Lycium barbarum* L. with an intraspecific F1 population, and 29 QTLs of photosynthetic traits were detected from 2-year 2017–2018 measurements and their mean data, together with three trunk diameter QTLs from 1 year 2018 data, all of them had low additive effects. Eight QTLs, including three P_N, two Cond, one Trmmol, one Ci, and one Ls-related QTL, can be detected with at least two datasets. qP_N1 was identified as a stable QTL for all 3 years datasets. Six photosynthetic traits also had QTLs that overlapped, and P_N and Cond were shown to have significant correlations with TD. We predicted that this work has laid a solid foundation for improving the breeding of goji to maximize the usage of photosynthesis with MAS, promoting the discovery of key genes controlling photosynthetic traits, and mapping of important agricultural traits.

Acknowledgments We also would like to thank Professor Kede Liu for his kind suggestions and help with the data analysis. We appreciated Bairuiyuan Company and Northwest Agriculture Research Center for their help with maintaining the goji orchard.

Funding information This work was supported by the National Key R&D Project of China (2018YFD1000607), a grant from the Chinese Academy of Sciences (XDA13020604), National Natural Science Foundation of China (31770334), Youth Innovation Promotion Association CAS (2015286), and Ningxia Agricultural Comprehensive Development Science and Technology Project (NTKJ2018-07).

Compliance with ethical standards

Conflict of interest The authors declare that they have no conflict of interest.

References

Akond M, Liu S, Schoener L, Anderson JA, Kantartzi SK, Meksem K, Song Q, Wang D, Wen Z, Lightfoot DA, Kassem MA (2013) A SNP-based genetic linkage map of soybean using the SoyS - NP6K Illumina Infinium BeadChip genotyping Array. Plant Genetics, Genomics, and Biotechnology 1:80–89

Amagase H, Farnsworth NR (2011) A review of botanical characteristics, phytochemistry, clinical relevance in efficacy and safety of *Lycium barbarum* fruit (Goji). Food Res Int 44: 1702–1717

Barria A, Christensen KA, Yoshida GM, Correa K, Jedlicki A, Lhorente JP, Davidson WS, Yanez JM (2018) Genomic predictions and genome-wide association study of resistance against Piscirickettsia salmonis in Coho Salmon (*Oncorhynchus kisutch*) using ddRAD sequencing. G3-Genes Genomes Genetics 8:1183–1194

Baxter SW, Davey JW, Johnston JS, Shelton AM, Heckel DG, Jiggins CD, Blaxter ML (2011) Linkage mapping and comparative genomics using next-generation RAD sequencing of a non-model organism. PLoS One 6:e19315

Brauer CJ, Unmack PJ, Beheregaray LB (2017) Comparative ecological transcriptomics and the contribution of gene expression to the evolutionary potential of a threatened fish. Mol Ecol 26:6841–6856

Catchen JM, Amores A, Hohenlohe P, Cresko W, Postlethwait JH (2011) Stacks: building and genotyping loci de novo from short-read sequences. G3-Genes Genomes Genetics 1:171–182

Chang RCC, Ho YS, So KF (2015) Wolfberry as anti-aging to prevent and delay neurodegeneration in Alzheimer's disease. In: International conference on food factors. ICoFF2015

Che Y, Song N, Yang Y, Yang X, Duan Q, Zhang Y, Lu Y, Li X, Zhang J, Li X, Zhou S, Li L, Liu W (2018) QTL mapping of six spike and stem traits in hybrid population of *Agropyron Gaertn* in multiple environments. Front Plant Sci 9

Chen YP, Chen YN, Li WH, Xu CC (2006) Characterization of photosynthesis of *Populus euphratica* grown in the arid region. Photosynthetica 44:622–626

Chen J, Liu X, Zhu L, Wang Y (2013) Nuclear genome size estimation and karyotype analysis of *Lycium* species (Solanaceae). Sci Hortic 151:46–50

Chen Z, Wang B, Dong X, Liu H, Ren L, Chen J, Hauck A, Song W, Lai J (2014) An ultra-high-density bin-map for rapid QTL

mapping for tassel and ear architecture in a large F-2 maize population. BMC Genomics 15:433

Chen J, Wang N, Fang L, Liang Z, Li S, Wu B (2015) Construction of a high-density genetic map and QTLs mapping for sugars and acids in grape berries. BMC Plant Biol 15:28

Chen WJ, Sun XF, Zhang RX, Xu MJ, Dou TH, Zhang XB, Zhong M, Yang WQ, Liu L, Lu XY, Zhu CQ (2017a) Hypertriglyceridemic acute pancreatitis in the emergency department: typical clinical features and genetic variants. J Dig Dis 18:359–368

Chen C, Xu M, Wang C, Qiao G, Wang W, Tan Z, Wu T, Zhang Z (2017b) Characterization of the *Lycium barbarum* fruit transcriptome and development of EST-SSR markers. PLoS One 12

Chen J, Chao CT, Wei X (2018) Gojiberry breeding: current status and future prospects. InBreeding and health benefits of fruit and nut crops 10. IntechOpen

DaCosta JM, Sorenson MD (2016) ddRAD-seq phylogenetics based on nucleotide, indel, and presence-absence polymorphisms: analyses of two avian genera with contrasting histories. Mol Phylogenet Evol 94:122–135

Dahech I, Farah W, Trigui M, Ben Hssouna A, Belghith H, Belghith KS, Ben Abdallah F (2013) Antioxidant and antimicrobial activities of *Lycium shawii* fruits extract. Int J Biol Macromol 60:328–333

Davey JW, Hohenlohe PA, Etter PD, Boone JQ, Catchen JM, Blaxter ML (2011) Genome-wide genetic marker discovery and genotyping using next-generation sequencing. Nat Rev Genet 12:499–510

Davik J, Sargent DJ, Brurberg MB, Lien S, Kent M, Alsheikh M (2015) A ddRAD based linkage map of the cultivated strawberry, Fragaria xananassa. PLoS One 10:e0137746

Fu B, Liu H, Yu X, Tong J (2016) A high-density genetic map and growth-related QTL mapping in bighead carp (*Hypophthalmichthys nobilis*). Sci Rep 6

Gong D, Huang L, Xu X, Wang C, Ren M, Wang C, Chen M (2016) Construction of a high-density SNP genetic map in fluecured tobacco based on SLAF-seq. Mol Breed 36

Han K, Lee HY, Ro NY, Hur OS, Lee JH, Kwon JK, Kang BC (2018) QTL mapping and GWAS reveal candidate genes controlling capsaicinoid content in Capsicum. Plant Biotechnol J 16(9):1546–1558

Harrington G (1979) Estimation of above-ground biomass of trees and shrubs in a *Eucalyptus-Populnea* F Muell woodland by regression of mass on trunk diameter and plant height. Aust J Bot 27:135–143

Herve D, Fabre F, Berrios EF, Leroux N, Al Chaarani G, Planchon C, Sarrafi A, Gentzbittel L (2001) QTL analysis of photosynthesis and water status traits in sunflower (*Helianthus annuus* L.) under greenhouse conditions. J Exp Bot 52: 1857–1864

Hund A, Ruta N, Liedgens M (2009) Rooting depth and water use efficiency of tropical maize inbred lines, differing in drought tolerance. Plant Soil 318:311–325

Kai W, Nomura K, Fujiwara A, Nakamura Y, Yasuike M, Ojima N, Masaoka T, Ozaki A, Kazeto Y, Gen K, Nagao J, Tanaka H, Kobayashi T, Ototake M (2014) A ddRAD-based genetic map and its integration with the genome assembly of Japanese eel (*Anguilla japonica*) provides insights into genome evolution after the teleost-specific genome duplication. BMC Genomics 15:233

Kakioka R, Kokita T, Kumada H, Watanabe K, Okuda N (2013) A RAD-based linkage map and comparative genomics in the gudgeons (genus *Gnathopogon, Cyprinidae*). BMC Genomics 14:32

Laila R, Park J, Robin AHK, Natarajan S, Vijayakumar H, Shirasawa K, Isobe S, Kim H, Nou I (2019) Mapping of a novel clubroot resistance QTL using ddRAD-seq in Chinese cabbage (*Brassica rapa* L.). BMC Plant Biol 19:13

Li S, Wang C, Chang X, Jing R (2012) Genetic dissection of developmental behavior of grain weight in wheat under diverse temperature and water regimes. Genetica 140:393–405

Li Y, Fan Y, Dai G, Qin K, Cao Y (2013) Cloning of *Lycium barbarum* Callase gene and expression analysis in male sterile material. Xibei Zhiwu Xuebao 33:437–443

Li B, Tian L, Zhang J, Huang L, Han F, Yan S, Wang L, Zheng H, Sun J (2014) Construction of a high density genetic map based on large-scale markers developed by specific length amplified fragment sequencing (SLAF-seq) and its application to QTL analysis for isoflavone content in *Glycine max*. BMC Genomics 15:1086

Li N, Yin Y, Wang F, Yao M (2018) Construction of a high-density genetic map and identification of QTLs for cucumber mosaic virus resistance in pepper (*Capsicum annuum* L.) using specific length amplified fragment sequencing (SLAF-seq). Breed Sci 68:233–241

Liu GF, Yang J, Xu HM, Hayat Y, Zhu J (2008) Genetic analysis of grain yield conditioned on its component traits in rice (*Oryza sativa* L.). Aust J Agric Res 59:189–195

Liu Z, Zhu H, Liu Y, Kuang J, Zhou K, Liang F, Liu Z, Wang D, Ke W (2016) Construction of a high-density, high-quality genetic map of cultivated lotus (*Nelumbo nucifera*) using next-generation sequencing. BMC Genomics 17

Long SP, Marshall-Colon A, Zhu X (2015) Meeting the global food demand of the future by engineering crop photosynthesis and yield potential. Cell 161:56–66

Migicovsky Z, Myles S (2017) Exploiting wild relatives for genomics-assisted breeding of perennial crops. Front Plant Sci 4(8):460

Mullet JE, Whitsitt MS (1996) Plant cellular responses to water deficit. Plant Growth Regul 20:119–124

Murray MG, Thompson WF (1980) Rapid isolation of high molecular-weight plant DNA. Nucleic Acids Res 8:4321–4325

Niklas KI (1995) Size-dependent allometry of tree height, diameter and trunk-taper. Ann Bot 75:217–227

Peterson BK, Weber JN, Kay EH, Fisher HS, Hoekstra HE (2012) Double digest RADseq: an inexpensive method for de novo SNP discovery and genotyping in model and non-model species. PLoS One 7:e37135

Phadnis N, Orr HA (2009) A single gene causes both male sterility and segregation distortion in *Drosophila* hybrids. Science 323:376–379

Pinheiro HA, DaMatta FM, Chaves A, Fontes E, Loureiro ME (2004) Drought tolerance in relation to protection against oxidative stress in clones of Coffea canephora subjected to long-term drought. Plant Sci 167:1307–1314

Qiu S, Chen J, Chen X, Fan Q, Zhang C, Wang D, Li X, Chen X, Chen X, Liu C, Gao Z, Li H, Hu Y (2014) Optimization of selenylation conditions for *Lycium barbarum* polysaccharide based on antioxidant activity. Carbohydr Polym 103:148–153

Qu M, Zheng G, Hamdani S, Essemine J, Song Q, Wang H, Chu C, Sirault X, Zhu X (2017) Leaf photosynthetic parameters

related to biomass accumulation in a global rice diversity survey. Plant Physiol 175:248–258
Rastas P (2017) Lep-MAP 3: robust linkage mapping even for low-coverage whole genome sequencing data. Bioinformatics 33:3726–3732
Richards RA (2000) Selectable traits to increase crop photosynthesis and yield of grain crops. J Exp Bot 51:447–458
Roche D (2015) Stomatal conductance is essential for higher yield potential of C-3 crops. Crit Rev Plant Sci 34:429–453
Rochette NC, Catchen JM (2017) Deriving genotypes from RAD-seq short-read data using stacks. Nat Protoc 12(12):2640–2659
Sanchez-Perez R, Dicenta F, Martinez-Gomez P (2012) Inheritance of chilling and heat requirements for flowering in almond and QTL analysis. Tree Genet Genomes 8:379–389
Schupbach T, Wieschaus E (1991) Female sterile mutations on the 2nd chromosome of Drosophila melanogaster. 2. Mutations blocking oogenesis or altering egg morphology. Genetics 129:1119–1136
Sinclair TR (2017) Water-conservation traits to increase crop yields in water-deficit environments case studies introduction. In: *Springerbriefs in Environmental Science*. Sinclair TR (ed). pp 1–3
Singh BD, Singh AK (2015) Marker-assisted plant breeding: principles and practices [M]. Springer, New Delhi
Solberg TR, Sonesson AK, Woolliams JA, Meuwissen THE (2008) Genomic selection using different marker types and densities. J Anim Sci 86:2447–2454
Stadler LJ (1931) The experimental modification of heredity in crop plants: I. induced chromosomal irregularities. Sci Agric 11:557–572
State Forestry Administration of China (SFAC) (2018) China Forestry Statistics yearbook-2017. China Forestry Publishing, Beijing
Sun X, Liu D, Zhang X, Li W, Liu H, Hong W, Jiang C, Guan N, Ma C, Zeng H, Xu C, Song J, Huang L, Wang C, Shi J, Wang R, Zheng X, Lu C, Wang X, Zheng H (2013) SLAF-seq: an efficient method of large-scale de novo SNP discovery and genotyping using high-throughput sequencing. PLoS One 8
Wang CC, Chang SC, Inbaraj BS, Chen BH (2010a) Isolation of carotenoids, flavonoids and polysaccharides from *Lycium barbarum* L. and evaluation of the antioxidant activity. Food Chem 120:184–192
Wang J, Hu Y, Wang D, Zhang F, Zhao X, Abula S, Fan Y, Guo L (2010b) *Lycium barbarum* polysaccharide inhibits the infectivity of Newcastle disease virus to chicken embryo fibroblast. Int J Biol Macromol 46:212–216
Wang N, Fang L, Xin H, Wang L, Li S (2012) Construction of a high-density genetic map for grape using next-generation restriction-site associated DNA sequencing. BMC Plant Biol 12:148
Wang S, Suh JH, Zheng X, Wang Y, Ho C (2017) Identification and quantification of potential anti-inflammatory hydroxycinnamic acid amides from wolfberry. J Agric Food Chem 65:364–372
Wang L, Zhou X, Ren X, Huang L, Luo H, Chen Y, Chen W, Liu N, Liao B, Lei Y, Yan L, Shen J, Jiang H (2018) A major and stable QTL for bacteria wilt resistance on chromosome B02 identified using a high-density SNP-based genetic linkage map in cultivated Peanut Yuanza 9102 derived population. Front Genet 9
Wu Z, Wang B, Chen X, Wu J, King GJ, Xiao Y, Liu K (2016) Evaluation of linkage disequilibrium pattern and association study on seed oil content in *Brassica napus* using ddRAD sequencing. PLoS One 11
Xu YB (2010) Molecular Plant Breeding. Oxfordshire, CABI Publishing
Xu X, Xu R, Zhu B, Yu T, Qu W, Lu L, Xu Q, Qi X, Chen X (2015) A high-density genetic map of cucumber derived from specific length amplified fragment sequencing (SLAF-seq). Front Plant Sci 5
Xu Y, Li S, Li L, Ma F, Fu X, Shi Z, Xu H, Ma P, An D (2017) QTL mapping for yield and photosynthetic related traits under different water regimes in wheat. Mol Breed 37
Yao R, Heinrich M, Zou Y, Reich E, Zhang X, Chen Y, Weckerle CS (2018) Quality variation of goji (fruits of *Lycium* spp.) in China: a comparative morphological and Metabolomic analysis. Front Pharmacol 9
Yin G, Dang Y (2008) Optimization of extraction technology of the *Lycium barbarum* polysaccharides by Box-Behnken statistical design. Carbohydr Polym 74:603–610
Zelitch I (1982) The close relationship between net photosynthesis and crop yield. Bioscience 32:796–802
Zhang L, Meng L, Wu W, Wang J (2015) GACD: integrated software for genetic analysis in clonal F-1 and double cross populations. J Hered 106:741–744
Zhang J, Long Y, Wang L, Dang Z, Zhang T, Song X, Dang Z, Pei X (2018) Consensus genetic linkage map construction and QTL mapping for plant height-related traits in linseed flax (*Linum usitatissimum* L.). BMC Plant Biol 18
Zhao X, Xu J, Zhao M, Lafitte R, Zhu L, Fu B, Gao Y, Li Z (2008) QTLs affecting morph-physiological traits related to drought tolerance detected in overlapping introgression lines of rice (*Oryza sativa* L.). Plant Sci 174:618–625
Zhao W, Chung J, Cho Y, Rha W, Lee G, Ma K, Han S, Bang K, Park C, Kim S, Park Y (2010) Molecular genetic diversity and population structure in *Lycium* accessions using SSR markers. Comptes Rendus Biologies 333:793–800
Zhao Q, Dong B, Chen J, Zhao B, Wang X, Wang L, Zha S, Wang Y, Zhang J, Wang Y (2015) Effect of drying methods on physicochemical properties and antioxidant activities of wolfberry (*Lycium barbarum*) polysaccharide. Carbohydr Polym 127:176–181
Zhou X, Xia Y, Ren X, Chen Y, Huang L, Huang S, Liao B, Lei Y, Yan L, Jiang H (2014) Construction of an SNP-based genetic linkage map in cultivated peanut based on large scale marker development using next-generation double-digest restriction-site-associated DNA sequencing (ddRADseq). BMC Genomics 15:351
Zhu Y, Yin Y, Yang K, Li J, Sang Y, Huang L, Fan S (2015) Construction of a high-density genetic map using specific length amplified fragment markers and identification of a quantitative trait locus for anthracnose resistance in walnut (*Juglans regia* L) BMC Genomics 16(1):614
Zhu J, Guo Y, Su K, Liu Z, Ren Z, Li K, Guo X (2018) Construction of a highly saturated genetic map for *Vitis* by next-generation restriction site-associated DNA sequencing. BMC Plant Biol 18(1):347